Journal of the Virtual Explorer, 2007
Volume 27
Paper 3
http://virtualexplorer.com.au/

The Geology of Ikaria Island:The Messaria extensional shear zone, granites and the exotic Ikaria nappe

Uwe Ring

Department of Geological Sciences
Canterbury University,
Christchurch 8140, New Zealand

Abstract: Abstract is not available.

Table of Contents

Prelude - Ikaria (area 265 km2, population about 7,500)

How Ikaria became its name

Daedalus was a highly respected and talented Athenian artisan descendent from the royal family of Cecrops, the mythical first king of Athens. He was known for his skill as an architect, sculpturer, and inventor and he produced many famous works. Despite his self-confidence, Daedalus once committed a crime of envy against Talus, his nephew and apprentice. Talus, who seemed destined to become as great an artisan as his uncle Daedalus, was inspired one day to invent the saw after having seen the way a snake used its jaws. Daedalus, momentarily stricken with jealousy, threw Talus off the Acropolis. For this crime, Daedalus was exiled to Crete and placed in the service of King Minos, where he eventually had a son, Icarus, with the beautiful Naucrate, a mistress-slave of the King.

Minos called on Daedalus to build the famous labyrinth for imprisoning the dreaded Minotaur. The Minotaur was a monster with the head of a bull and the body of a man. He was the son of Pasiphae, the wife of Minos, and a bull that Poseidon had sent to Minos as a gift. Minos was shamed by the birth of this horrible creature and decided to imprison the Minotaur in the labyrinth where it fed on humans, which were taken as "tribute" by Minos and sacrificed to the Minotaur in memory of his fallen son Androgenos.

Theseus, the heroic King of Athens, volunteered himself to be sent to the Minotaur in the hopes of killing the beast and ending the ‘human tribute’ that his city was forced to pay Minos. When Theseus arrived in Crete, Ariadne, Minos's daughter, fell in love with him and wished to help him survive the Minotaur. Daedalus revealed the mystery of the labyrinth to Ariadne who in turn advised Theseus, thus enabling him to slay the Minotaur and escape from the labyrinth. When Minos found out what Daedalus had done he was so enraged that he imprisoned Daedalus and Icarus in the labyrinth themselves.

Daedalus conceived to escape from the labyrinth with Icarus by constructing wings and then flying to safety (Figure 1). He built the wings from feathers and wax, and before the two set off he warned Icarus not to fly too low lest his wings touch the waves and get wet and not too high lest the sun melt the wax. But the young Icarus, overwhelmed by the thrill of flying, did not heed his father's warning, and flew too close to the sun whereupon the wax in his wings melted and he fell into the sea. Daedalus escaped to Sicily and Icarus' body was carried ashore by the current to an island then without a name. Heracles came across the body and recognized it, giving it burial where today there still stands a small rock promontory jutting out into the Aegean Sea, and naming the island and the sea around it after the fallen Icarus.

Figure 1. Icarus and Deadalus

Icarus and Deadalus

History

Ikaria (Icaria), Icarus in classical antiquity, is a member of the Anatolian Sporades, and is part of the same mountain range, which connected Samos to Asia Minor. Ikaria has nearly an unbroken coastline, and is without adequate ports. The sea around Ikaria, the Ikarian Pelagos, was known to Homer (Iliad 2, p.145) as one of the most turbulent areas of the Aegean. The Ikarian Sea is especially tempestuous in July and August during the meltimi season because the island, situated without a protective barrier to the

north, has no buffer from these northeasterly gales known as Etesian in antiquity.

There are some neolithic remains on Ikaria that are presently being excavated by a native, Themistocles Katsaros. Another native, the eminent anthropologist Ares Poulianos, has found a number of neolithic artifacts. Ikaria was inhabited in the seventh millennium B.C. and the Greeks called these early inhabitants of the Aegean Pelasgians. The Pelasgians probably controlled Ikaria until the second millennium B.C. when the Carians, another indigenous Aegean people, got a foothold in Ikaria. These terms, Pelasgians and Carians are very vague and it is perhaps best to simply think of the early settlers of Ikaria as pre-Greek.

The Greeks entered the Aegean in ca. 1500 B.C., and by 1200 B.C. had taken most of the Aegean islands, though there is no sign of any Greek settlement on Ikaria until much later. The Greeks may have been discouraged by the lack of harbors, the shortage of arable land and thick forests. Greeks from Miletus colonised Ikaria in 750 B.C, probably establishing a settlement at Therma and later at Oenoe (which today is called Kampos). The purpose of these Milesian outposts on Ikaria was probably to aid Milesian ships on their way north to Milesian colonies in the Propontis.

The sources for the history of ancient Ikaria consist of random references by ancient authors such as Thucydides, Herodotus, Strabo, Pausanias, Athenaeus, Pliny, and a handful of inscriptions. Eparchides, a native of Oenoe, wrote a history of Ikaria about 350 B.C. and it is assumed that he provided a capsule history of the island, but the main purpose of his work seems to have been to promote Ikarian wine. Only several fragments of Eparchides' history survive.

Sometime in the 6th century B.C. Ikaria was absorbed by Samos and became part of Polycrates sea-empire. It was perhaps at this time that the temple of Artemis at Nas, on the northwest coast of the island was built. It seems that Nas was a sacred place to the pre-Greek inhabitants of the Aegean, and an important port in the Aegean, the last stop before sailing the dangerous Ikarian Sea. It was an appropriate place for sailors to make sacrifices to Artemis, who among other functions was a patron of seafarers. The temple was pillaged in the 19th century by the villagers of Christos Raches for marble for their local church. In 1939 it was excavated by the Greek archeologist Leon Politis. During the German and Italian occupation of Ikaria in World War II many of the artifacts unearthed by Politis disappeared. Local custom has it that there are still marble statues embedded in the sand off the coast.

In the first decades of the 5th century Ikaria may have fallen into the sphere of Persia. In 490 B.C. the Persian expeditionary force to Greece touched upon Ikarian shores. After the war Ikaria became part of the Delian League and prospered. Oenoe became known for its excellent Pramnian Wine. There were several areas in Greece which produced this type of wine, which seems to have been rather expensive and enabled Oenoe to pay a substantial tribute to the Athenians. The record of this tribute is the aparachai, the tribute list kept in Athens, which shows Oenoe paying 8,000 drachmae in 453 B.C., dropping to 6,000 in 449 B.C., and 4,000 in 448 B.C. A drachma was a substantial sum in the ancient world, and the total Ikarian tax placed Ikaria in the upper thirty percent of the tribute paying states.

Therma apparently did not share in the great wine industry and apparently had little to do with Oenoe. There are no records that the two Ikarian cities had much contact. This division is reflected in the modern period when in 1912 the two sections of the island almost went to war with one another to determine the site of the capital. Therma's prosperity seems to have been based on its thermal springs which even then were considered highly beneficial.

It was estimated that about 13,000 inhabitants lived on Ikaria in the 5th century B.C. The prosperity, which the island enjoyed during the Athenian empire, began to decline during the Peloponnesian War (431 B.C. to 404 B.C.). On two occasions Spartan admirals, Alcidas and Mindarus, brought their fleets to Icaria. After the war Ikaria suffered from piratical raids. Conditions improved in 387 B.C. when Ikaria, that is Oenoe and Therma, became a member of the Second Athenian League.

Alexander the Great named an island in the Persian gulf (Failaka) Ikaria because it resembled Ikaria. In fact, there is no resemblance between the two islands and it is unknown why Alexander would do this, but his gesture does signify that he held Ikaria in some degree of esteem and perhaps had soldiers from the island in his Persian campaign. In the wars that followed the death of Alexander in 323 B.C., Ikaria became an important military base. One of Alexander's successors, possibly Demetrius Poliorcetes, built the tower at Fanari, Dracanum, and the adjacent fortress. It is one of the best preserved Hellenistic military towers in the Aegean (Figure 2).

Figure 2. Dracanum

The tower northeast of Fanari.

In the 2nd century B.C. the Ikarians changed the name of Therma to Aslcepieis. The change in names only lasted for about thirty years. Apparently, it was an effort to advertise the medicinal qualities of the thermal baths and to make Therma into an important resort. The 2nd century B.C. was, in general, a period of decline. Philip V (221 B.C. - 178 B.C.) ravaged the Aegean islands. Though the Romans established control of the area they did not adequately patrol the seas. In 129 B.C. Samos was incorporated into the Roman province of Asia, which represented a coastal area of Asia Minor, and Ikaria seems to have been included in this province. A Roman general undertook to repair the temple of Artemis which had apparently fallen into a state of disrepair during the 3rd century B.C, doubtless from piratical raids, but the Romans, preoccupied by domestic problems, neglected the Aegean and by the early years of the 1st century B.C. pirates took control of the Aegean islands. All the coastal settlements in Ikaria disappeared and the few people who remained on the island retreated into the interior. The Emperor Augustus (29 B.C. - A.D. 14) reestablished order in the Aegean and encouraged Samians to develop Ikaria. The traveler Strabo, ~10 B.C., saw two small settlements on Ikaria, but noted that it was essentially a deserted island used mainly by Samian farmers who kept herds of animals there. In the 1st century A.D. Pliny the Younger was weather bound on the island for several days and was struck by its rustic qualities.

By the end of the 5th century A.D. Ikaria fell into the sphere of the Byzantine Empire. Kampos, the former Oenoe, became the administrative center and the seat of a bishopric. The Samians, given support by the government in Constantinople, maintained a local fleet which offered Ikaria some protection from pirates. In 1081 A.D. the emperor Alexus Comnenus established only a few miles from Ikaria the monastery of St. John the Theologian in Patmos. This became a cultural center in the Aegean and kept Ikaria from sliding into total oblivion.

By the end of the 12th century the Byzantine empire cut back its naval defense and the Aegean became open to inroads from pirates and Italian adventures. The Ikarians built fortresses at Paliokastro and Koskino. A glimpse of conditions is provided by a document in the monastery of Patmos which recorded pirates fleeing Patmos and arriving in Ikaria where the local population executed them.

In the 14th century the Genoese took Chios, and Ikaria became part of a Genoese Aegean empire. When the Turks drove the Genoese from the Aegean the Knights of St. John, who had their base in Rhodes, exerted some control over Ikaria until 1521 when the Sultan incorporated Ikaria into his realm. The Ikarians killed the first Turkish tax collector, but somehow managed to escape punishment. The Turks imposed a very loose administration not sending any officials to Ikaria for several centuries. The best account we have of the island during these years is from the pen of the bishop J. Georgirnees who in 1677 described the 1,000 inhabitants of the island as the poorest people in the Aegean. In 1827 Ikaria broke away from the Ottoman Empire, but was forced to accept Turkish rule a few years later, and remained part of the Ottoman empire until 17 July 1912 when it expelled a small Turkish garrison during the Ikarian independence. Due to the Balkan Wars Ikaria was unable to join Greece until November of that year. The five months of independence were difficult years. The natives lacked food, were without regular transportation and postage

service, and were on the verge of becoming part of the Italian Aegean empire.

The island suffered tremendous losses in property and lives during the World War II and the German and Italian occupation. There are no exact figures on how many people starved, but in the village of Karavostomos over 100 perished from starvation. After the war the majority of the islanders were sympathetic to communism and the Greek government used the island to exile about 13,000 communists from 1945 to 1949. There was considerable dissatisfaction with the Greek government which invested little in developing Ikaria which remained one of the most backward regions of Greece. Until the 1960's the Ikarians looked to the Ikarians in America rather than Athens for help in building roads, schools and medical facilities. Throughout the first half of the 20th century the economy depended on remittances sent from the US by Ikarian immigrants who began settling in America in the 1890's. In the US Ikarians demonstrated a talent as steel mill workers and independent business men. The quality of life improved after 1960 when the Greek government began to invest in the infrastructure of the island and assisted in the promotion of tourism.

Introduction

The extending Hellenide orogen in the Aegean Sea of Greece (Figure 3) exposes a number of spectacular brittle low-angle normal faults (detachments) (Lister et al. 1984; Lee & Lister 1992). On some Aegean islands, the brittle detachments are associated with underlying extensional ductile shear zones and examples of these ductile-to-brittle extensional fault systems have been reported from the Cycladic islands of Naxos (Buick 1991) and Ios (Vandenberg & Lister 1996). Another well-exposed but little known example is the Messaria extensional fault system on Ikaria Island, which has been described in some detail by Christine Kumerics (Kumerics et al. 2005). Extension was accompanied by the intrusion of three granites: the large I-type Raches granite occupying the western half of the island, the smaller S-type Karkinagrion granite, which occurs within the I-type Raches granite, and the smaller S-type Xylosirtis granite at the south coast (Figure 4). The footwall of the Messaria extensional shear zone is the Ikaria nappe, which seems to be a rather exotic nappe in the central Aegean which apparently is only exposed on Ikaria and has no counterpart on the adjacent Aegean island. The Ikaria nappe may correlate to nappes on the nearby Turkish mainland.

Figure 3. Generalized map

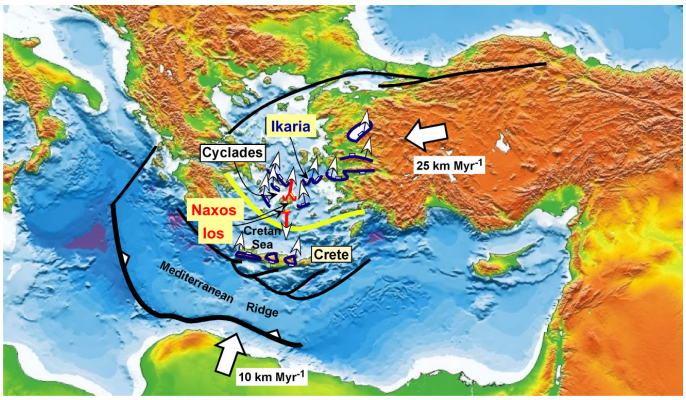

Generalized map of the Aegean and adjacent mainlands showing tectonometamorphic units and Hellenic subduction zone. Inset shows the location of the main map.

Figure 4. Simplified geological map of Ikaria Island

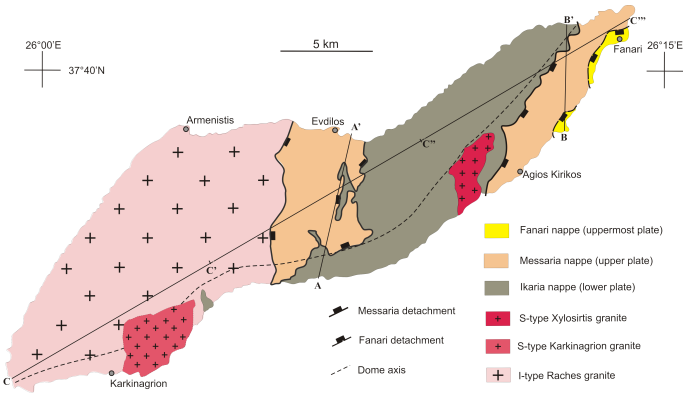

Simplified geological map of Ikaria Island. Shown are tectonic units, the Messaria and Fanari extensional detachments, the localities of structural, strain, geochronological and P-T samples, the positions of two cross sections A-A' and B-B' shown in Fig. 3, cross section C-C'-C''-C''' shown in Fig. 12, and profiles D-D' and E-E' for the slip-rate calculations in Fig. 17.

Setting

Previous research has distinguished several tectonic zones in the Hellenides characterised by rock type, stratigraphy, tectonometamorphic history and pre-orogenic palaeogeography (Robertson et al. 1991). The Cycladic blueschist unit is the dominant tectonic unit in the central Aegean and represents the most deeply exhumed unit in the entire region. The Cycladic blueschist unit comprises from

top to bottom three composite nappes: (1) an ophiolitic mélange; (2) a Permo-Carboniferous to latest Cretaceous passive-margin sequence, and (3) a Carboniferous basement, which also occurs as slices in the passive-margin sequence (see Ring et al., this volume, for schematic of structural pile). The Cycladic blueschist unit is overlain on some islands by the Upper unit, which is a non- to weakly metamorphosed ophiolitic nappe that contains Pliocene sediments. In some windows in the Cycladic zone, the Basal unit, as part of the External Hellenides, crops out below the Cycladic blueschist unit (Godfriaux 1968; Avigad & Garfunkel 1989). The Cycladic blueschist unit and the External Hellenides were part of the Adriatic microcontinent. A major difference between the Aegean and adjacent western Turkey is that in the latter the Menderes nappes instead of the External Hellenides form the lowermost tectonic unit. In contrast to parts of the External Hellenides, the Menderes nappes do not show Tertiary high-pressure metamorphism (Gessner et al. 2001; Ring et al. 2001; Régnier et al. 2003). The Menderes nappes are part of the Anatolian microcontinent, which collided with Eurasia further east than Adria (Figure 5). A distinctive feature of the Anatolian microcontinent is that its basement formed at ~550 Ma (Gessner et al. 2001, 2004; Ring et al. 2004).

Figure 5. Palaeogeographic sketch

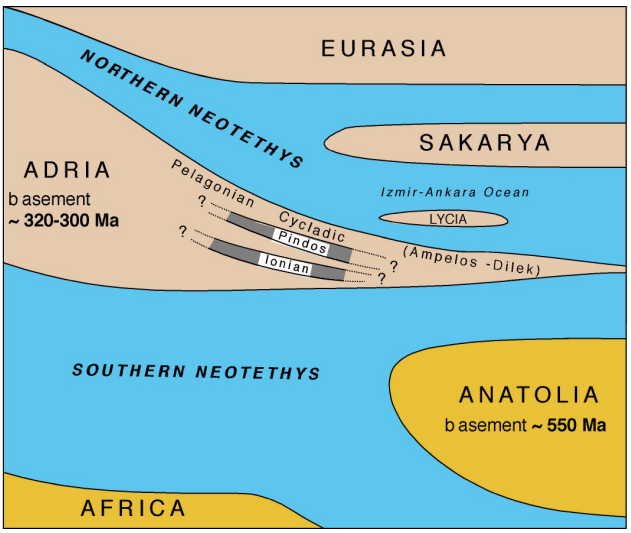

Palaeogeographic sketch outlining the complex geometry of the Adriatic and Anatolian plates.

The metamorphic evolution of the Cycladic blueschist unit includes an Early Tertiary high-pressure event (~15-20 kbar and 500 ± 50°C) at ~55-45 Ma followed by one or more greenschist-facies overprints (~4-7 kbar and 400 ± 50°C on most islands; the amphibolite-facies overprint on Naxos Island is exceptional) (Altherr et al. 1982; Wijbrans et al. 1990; Tomaschek et al. 2003; Ring & Layer 2003). High-pressure metamorphism in the Basal unit on Evia and Samos islands is dated at 24-21 Ma (Ring & Reischmann 2002).

In the Middle to Late Miocene, the Cyclades became part of the magmatic arc of the southward retreating Hellenic subduction zone as evidenced by arc-related volcanic rocks ranging from ~11-6 Ma (Fytikas et al. 1984; Weidmann et al. 1984) and granites spanning an age range from ~14-10 Ma (Keay 1998). The granites were emplaced synkinematically during extensional faulting (Faure et al. 1991; Lee & Lister 1992).

Geology and architecture of Ikaria Island

Three tectonic units can be distinguished on the island of Ikaria; they are from top to bottom: (a) the non-metamorphosed Fanari nappe; (b) the Messaria nappe (including the Kefala unit) and (c) the Ikaria nappe (Figs 4, 6). The general structure of Ikaria is dominated by a ~300-500 m thick ductile extensional shear zone, the Messaria shear zone, and two associated brittle detachment faults, the Messaria and Fanari detachments. The Messaria detachment is the upper crustal expression of the ductile Messaria shear zone. In the reminder of this field trip guide we refer to this detachment/shear-zone system as the Messaria extensional fault system. The Fanari detachment is not associated with an underlying ductile shear zone. The Messaria and Ikaria nappes are separated from one another by the Messaria detachment; the Messaria shear zone developed in the upper parts of the Ikaria nappe. The Fanari detachment separates the Messaria nappe from Pliocene conglomerates of the Fanari nappe.

The island has an asymmetric dome-shaped architecture (Figs 4, 6, 7). The northwestern slopes of the island dip gently to the north, which mimics the shallow northern dip of the Messaria extensional fault system (Figure 7). The southern slopes of Ikaria Island dip much more steeply to the south (Figure 8).

Figure 6. Cross sections A-A' and B-B'

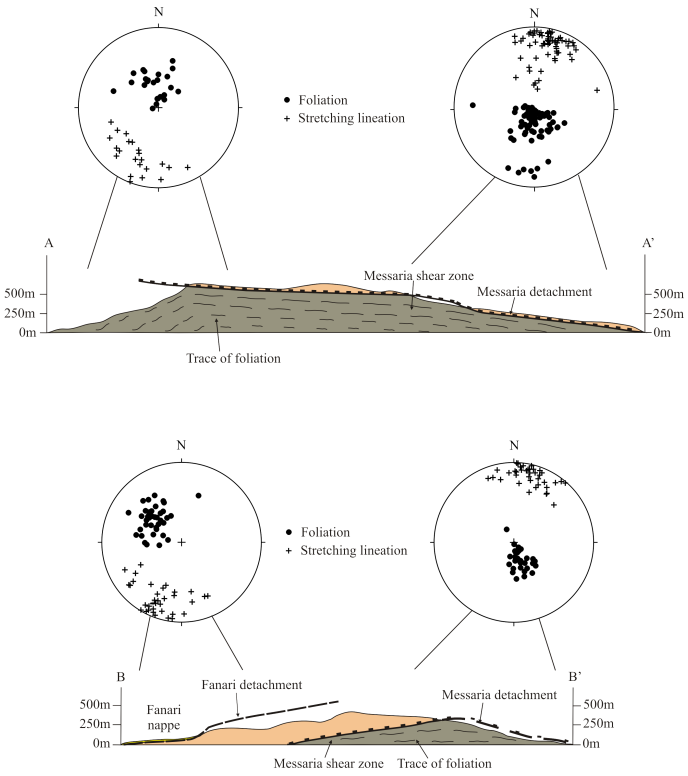

Cross sections A-A' and B-B' illustrating domed architecture, which is also expressed by dip and plunge of foliations and stretching lineations on both sides of Ikaria Island.

Figure 7. I-type Raches granite

View on the I-type Raches granite showing gently sloping north side in the upper part of the photograph and abrupt drop at south coast in lower right. The plain area in the centre of the photograph essentially mimics the shallow dip of the Ikaria shear zone.

Figure 8. Steep slopes

Steep slopes at the south coast of Ikaria Island.

The Pliocene conglomerates of the Fanari nappe, which is part of the Upper unit of the Cycladic zone, contain pebbles of metamorphic rocks, which are not exposed on Ikaria Island (Dürr et al. 1978).

The Messaria nappe comprises metabauxite-bearing marble, graphite-rich calc-mica schist, chloritoid-kyanite-bearing phyllite, quartzite and greenschist (Altherr et al. 1982). The marble in places contains small serpentinite lenses (Figure 9). Structural position and lithology indicate that the Messaria nappe correlates with the Ampelos nappe on nearby Samos Island (Ring et al. this volume). Both nappes are part of the passive-margin sequence of the Cycladic blueschist unit. Will et al. (1998) estimated peak pressure-temperature (P-T) conditions of ~15 kbar and ~500°C for the Ampelos nappe on Samos Island (see also Ring et al. this volume) and we regard these estimates as a reasonable approximation for high-pressure P-T conditions in the Messaria nappe. The Kefala unit is a klippe of marbles (with upper Triassic fossils) that makes up a small patch in the central part of Ikaria north of Evdilos (Figure 10).

Figure 9. serpentine lenses

Small, asymmetric serpentine lenses in marble of Messaria nappe.

Figure 10. Klippe of Kefala marble

Klippe of Kefala marble in centre of photograph. Note also marked asymmetry in morphology with gently sloping northern part of the island to the right and steeply dipping south side to the left.

The Ikaria nappe at the base is more than 1000 m thick and consists of a huge succession of metapelite as well as minor marble, calcsilicate rocks, amphibolite, quartzite and metapegmatite. The Ikaria nappe was intruded by three synkinematic granites: the large I-type Raches granite in the west (Figure 7), the S-type Karkinagrion granite and the small S-type Xylosirtis granite in the southern part of the island (Figure 4). The metapelite contains the amphibolite-facies mineral assemblage garnet-kyanite-staurolite-biotite-plagioclase (Altherr et al. 1982). An important question is whether the Ikaria nappe shows evidence for pre-amphibolite-facies high-pressure metamorphism, which is typical for the nappes of the Cycladic blueschist unit. If so, the P-T evolution of the Ikaria nappe would generally be comparable to that of the Carboniferous basement of the Cycladic blueschist unit on Naxos Island with its exceptional amphibolite-facies Miocene metamorphism. Alternatively, the Ikaria nappe might be an exotic non-high-pressure unit in the Aegean and would probably correlate with the Menderes nappes of western Turkey.

Metamorphism of the Ikaria nappe and its tectonic implications

P-T conditions for the Ikaria unit (see stops 3.1 and 3.4 below for details of samples) were estimated via pseudosections using the KFMASH system based on whole-rock analyses and constrain P-T estimates for IK02-06a at 6-8 kbar for a temperature of 600-650°C and >6-<7 kbar for IK02-16 (Figure 11).

Figure 11. Pseudosections and AFM diagrams

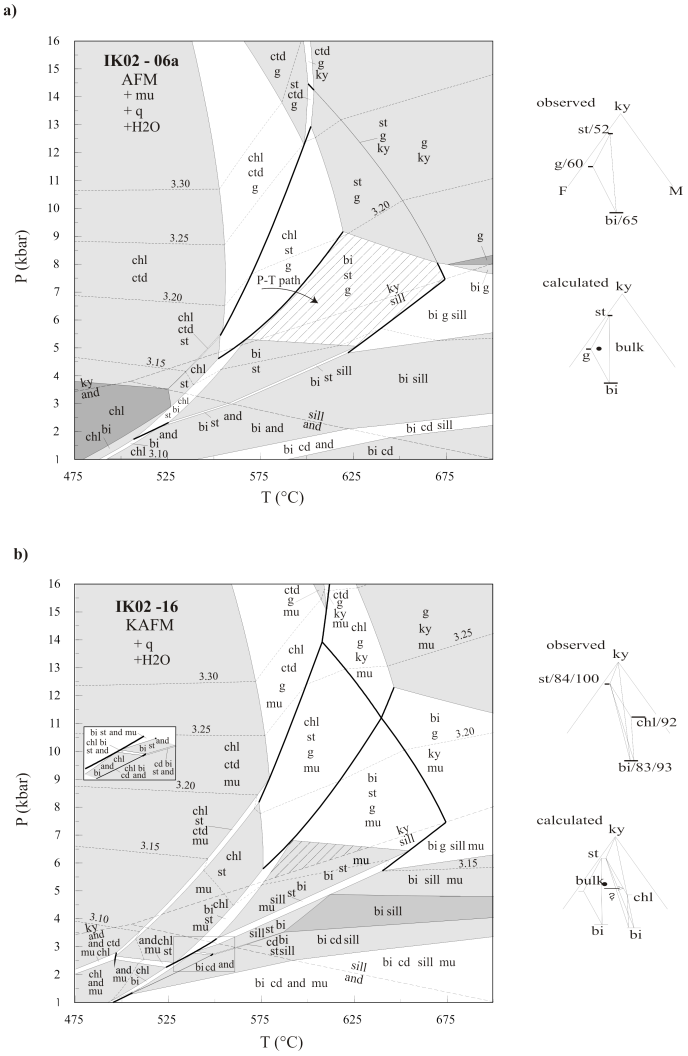

Pseudosections and AFM diagrams; phengitic substitution in white mica is shown by dashed lines in both pseudosections; the projection of the bulk-rock composition is labelled bulk for both samples in the AFM diagrams. (a) Sample IK02-06a; projections into an AFM diagram are based on mineral formulae of muscovite (pure end member), quartz and water; same projections calculated by THERMOCALC are also shown; inferred pressure is 6-8 kbar for a temperature of 600-650°C (hatched field in pseudosection); a possible P-T path is shown.

(b) Sample IK02-16; projections based on mineral formulae (observed) and calculated by THERMOCALC are shown; P-T conditions of 6 kbar and 600°C (hatched field in pseudosection) are indicated. Abbreviations: bi = biotite, cd = cordierite, chl = chlorite, ctd = chloritoid, ep = epidote, fsp = plagioclase, g = garnet, ky = kyanite, and = andalusite, sill = sillimanite, mu = muscovite, q = quartz, st = staurolite.

A very important conclusion is that there is no evidence for any high-pressure metamorphism pre-dating amphibolite-facies metamorphism in samples IK02-6a and IK02-16 from the Ikaria nappe. Reconnaissance metamorphic analyses of other samples from the Ikaria nappe also do not show any signs for high-pressure relics. Altherr et al. (1982) also did not report any evidence for high-pressure metamorphism in the Ikaria nappe.

The absence of any sign of high-pressure metamorphism suggests that the Ikaria nappe does not belong to the Cycladic blueschist unit and might in fact be an exotic non-high-pressure unit in the Aegean. To which tectonic unit does the Ikaria nappe then belong? The only mid-amphibolite-facies units, which have no Tertiary high-pressure overprint in the region are the Çine and Bozdağ nappes of the Menderes nappes of western Turkey (Ring et al. 1999a; Gessner et al. 2001; Régnier et al. 2003). Large parts of the Çine nappe consist of ~550 Ma old augengneiss, which does not occur in the Ikaria nappe. We tentatively correlate the Ikaria nappe with the Bozdağ nappe of western Turkey, which also comprises a very thick metapelite sequence and minor marble, amphibolite and quartzite (Ring et al. 2001). The Çine and Bozdağ nappes belong to the lowest tectonic unit (Menderes nappes) of western Turkey, which was overthrust by the Cycladic blueschist along the Cyclades-Menderes thrust unit in the Eocene (Gessner et al. 2001). We speculate that the Cyclades-Menderes thrust emplaced the Messaria nappe onto the Ikaria nappe.

Our correlation of the Ikaria nappe with the Bozdağ nappe of the Menderes nappes results in a major geometric problem in the eastern Aegean. On Samos Island east of Ikaria, the Cycladic blueschist unit rests on the Basal unit (External Hellenides), which in general makes up the lowest tectonic unit in the Aegean (see Ring et al. this volume). If the Ikaria nappe indeed belongs to the Menderes nappes it would have been derived from Anatolia (Figure 5) and this implies that the interfingering of Adria and Anatolia has a complex geometry in the eastern Aegean.

The Messaria shear zone and the three granites

The stretching lineations associated with extensional shearing in the Messaria shear zone (Figure 12) show a consistent NNE-SSW orientation; the lineations plunge to the north in the northern part of the island and to the south in the southeastern part (Figure 6) and (Figure 13). Shear bands associated with the stretching lineations in the Messaria shear zone consistently indicate a top-to-the-NNE sense of shear (Figure 14). The shear bands developed during greenschist-facies metamorphism and the amphibolite-facies mineral assemblages in the Ikaria nappe were completely retrograded in the shear zone. In incipiently sheared rocks, asymmetric strain shadows around garnet contain chlorite, white mica and quartz and developed during garnet break down. Biotite is converted to chlorite in the shear bands. Staurolite breaks down to white mica and chlorite. In highly sheared rocks, relics of amphibolite-facies parageneses are lacking and the mylonite is made up of greenschist-facies mineral assemblages. In the Messaria nappe, kyanite and chloritoid in weakly sheared rocks have cracks that are filled with chlorite and quartz. Rare biotite is strongly chloritised. Mylonitic rocks usually have ribbon quartz and rotated albite porphyroclasts.

Figure 12. Quartzitic schist

Quartzitic schist with well developed stretching lineation.

Figure 13. Messaria shear zone

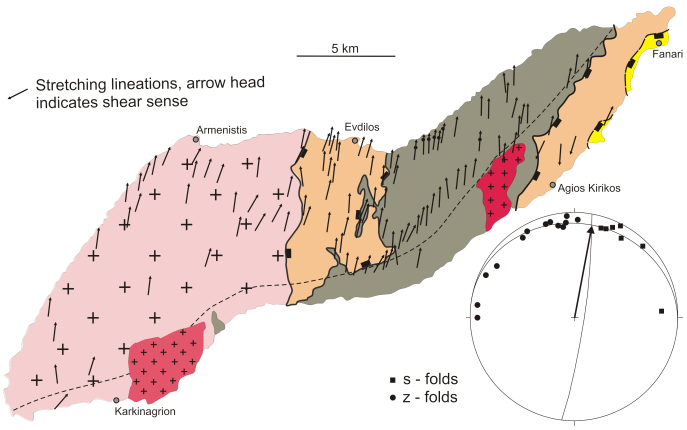

(a) Map showing orientation of stretching lineations; arrowhead indicates shear sense of hangingwall. (b) Stereogram showing asymmetric folds in Messaria shear zone. The sense of asymmetry is assigned on the basis of fold vergence when viewed in the down-plunge direction. The axis and sense of asymmetry of each fold is plotted in a lower-hemisphere projection according to the convention of Cowan & Brandon (1994). The fold axes define a girdle, which parallels the orientation of the shear plane; the fold axes plot as two distinct "S" and "Z" groups. The shear direction for the shear zone can be determined from the intersection of the shear plane (average girdle of "S" and "Z" axes) and the mirror plane; the shear direction is top-to-the-NNE.

Figure 14. top-N sense of shear

Photographs illustrating the top-N sense of shear within the Ikaria shear zone.

Large parts of the I-type Raches granite in the southwestern corner of Ikaria are virtually undeformed and exhibit magmatic fabrics. Aligned igneous minerals of euhedral potassium feldspar, plagioclase, biotite and hornblende in an undeformed quartz matrix define a magmatic foliation. Thin-section analysis shows that the minerals forming the magmatic foliation do not show any signs of deformation or recrystallisation. In the upper parts of the granite, the magmatic foliation has a subhorizontal orientation. Here a weak NNE-trending magmatic lineation is defined by preferred orientation of the long axes of prismatic potassium feldspar. In its uppermost parts, the I-type granite is progressively deformed into mylonite and ultramylonite with a subhorizontal tectonic foliation associated with a very strong NNE-trending stretching lineation. The mylonitic foliation is defined by medium- to fine-grained flattened and strongly elongated quartz grains, quartz-feldspar aggregates and aligned mica. The foliation may be spaced at the millimetre scale or is extremely narrowly spaced at the micron scale. The lineation is expressed by stretched quartz-mica aggregates and recrystallised quartz tails around feldspar porphyroclasts. Quartz commonly forms polycrystalline ribbons and shows undulatory extinction, dynamic recrystallisation and grain-boundary migration. Micas are commonly recrystallised into small new grains, which define C planes that lie at a small angle to the mylonitic foliation.

The smaller S-type Karkinagrion granite occurs within the large I-type Raches granite on the southwest coast of Ikaria (Figure 4). The Karkinagrion granite has in places a weak, steeply dipping magmatic foliation, which is overprinted by a similarily oriented tectonic foliation.

The S-type Xylosirtis granite shows basically the same structural development as the I-type Raches granite and we argue that all three granites were intruded synkinematically into the Messaria shear zone.

In the Messaria shear zone numerous folds occur (Figure 15). Some of these shear-zone-related folds are strongly asymmetric on the dm to m scale. The asymmetry of the folds is consistent with top-to-the-NNE shear. The shear direction as deduced from the asymmetric folds is consistent with the orientation of the stretching lineations (Figure 13b). The ductile structures show a progressive evolution into semi-ductile and brittle structures associated with the brittle Messaria detachment. The detachment zone is made up of brecciated cataclasite in which rocks from the foot- and hangingwall are intermixed. In the Messaria nappe, marble is brecciated and jointed. Faults with offsets on the 10-100 m scale subdivide the marble into a number of tilted blocks in the hangingwall of the detachment. The sense of tilting is consistent with top-to-the-NNE displacement. Fault-slip analysis on faults in the Messaria nappe also indicates a consistent NNE-SSW-oriented extension direction (Figure 16). Throughout the upper parts of the I-type Raches granite, potassium feldspar porphyroclasts and hornblende show brittle micro-normal faults at moderate to high angles to the mylonitic foliation. These microfaults are commonly pulled apart feldspar and hornblende and growth of new quartz and biotite occurred between the displaced crystal fragments. Directly underneath the detachment fault, granite mylonite is brecciated and fractured and cataclasite and ultracataclasite occur. Very fine-grained retrograde chlorite is common in the breccia zones and feldspar is severely altered to sericite.

Figure 15. Refolded isoclinal folds

Refolded isoclinal folds in metapelite of Messaria shear zone.

Figure 16. Fault-slip analysis.

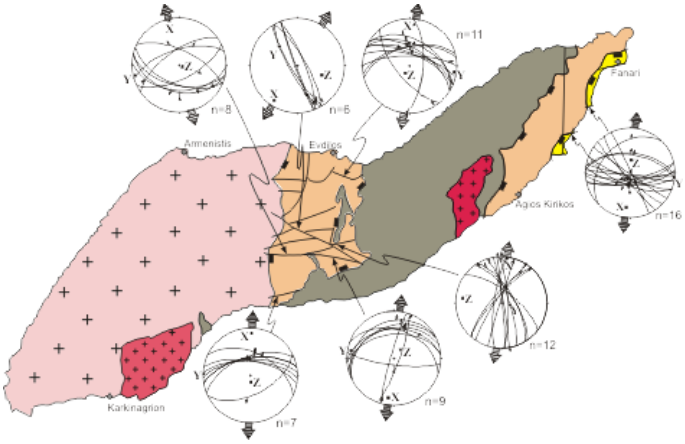

Fault-slip analysis. Most small-scale faults associated with the Messaria detachment dip at angles of 30-60° to the NNE; S-dipping normal faults are distinctly steeper than N-dipping ones. NE-striking strike-slip faults are dextral and NW-striking ones are sinistral. The large arrows indicate the calculated extension directions.

Locally open folds with subhorizontal N-S-trending axes (Figure 17) fold the detachment-related stretching lineations and also appear to affect the Messaria detachment. In places, the fold hinges of these folds are decorated with ~E-W-striking extension veins and fibres in those veins trend NNE-SSW. We therefore interpret these folds as late-stage, detachment-related folds that accommodated a very limited amount of ~E-W shortening associated with NNE-directed extension.

Figure 17. Late asymmetric fold

Late asymmetric fold, view is to the south.

The Fanari detachment at the contact between the Messaria and the Fanari nappe is a cataclasite zone. The cataclastic rocks have a rubbly to fragmental appearance and show numerous mesoscopic brittle faults. The fault planes are characterized by anastomosing clayey and carbonatitic gouge layers with thin (1 mm to 10 cm) zones of cataclasite, breccia and hematite-clay-coated fractured rock. Bleaching and alteration of intact rock occurs in the vicinity of faults. Weakly oriented phacoid-shaped tectonic slivers of country rock within the fault zone are on the cm to dm scale. The fault surfaces contain Riedel shears associated with lunate and crescentric structures at their intersections with the fault plane. The cataclastic fabrics record a top-to-the-NNE sense of shear. The cataclastic shear zone of the Fanari detachment is dissected by numerous small-scale faults. Fault-plane analysis shows that most of these faults have a normal sense of slip and dip at 50-70° to the south; a minor, conjugate set of normal faults dips at 60-80° to the N (Figure 16).

Strain and rotation analysis

For her PhD thesis, Christine Kumerics worked in detail on the strain and rotation history of the Messaria shear zone and most of her data are reported in Kumerics et al. (2005). Here we summarise the major results of her work only. The Flinn diagram in (Figure 18) shows the relative shapes of the strain ellipsoids, i.e. prolate vs oblate. As shown in (Figure 18), Fry strains are not fundamentally different from Rf/Φ strains; in some cases, the Rf/Φ strains are slightly greater than the Fry strains, whereas in other cases the opposite is the case. Therefore, we conclude that there was no significant difference in deformation behaviour between the matrix and the porphyroclasts during the accumulation of finite strain. The strain ellipsoids have mostly oblate strain symmetry with some data points in the prolate field (Figure 18). The axial ratios in XZ sections range from 2.4 to 19.9 with SX ranging from 1.2 to 7.2. The stretches in the Z direction, SZ, range from 0.3 to 0.6, indicating strong vertical shortening of 40% to 70%. SY ranges from 0.9 to 1.6, showing mainly extension in this direction.

Figure 18. Flinn diagram

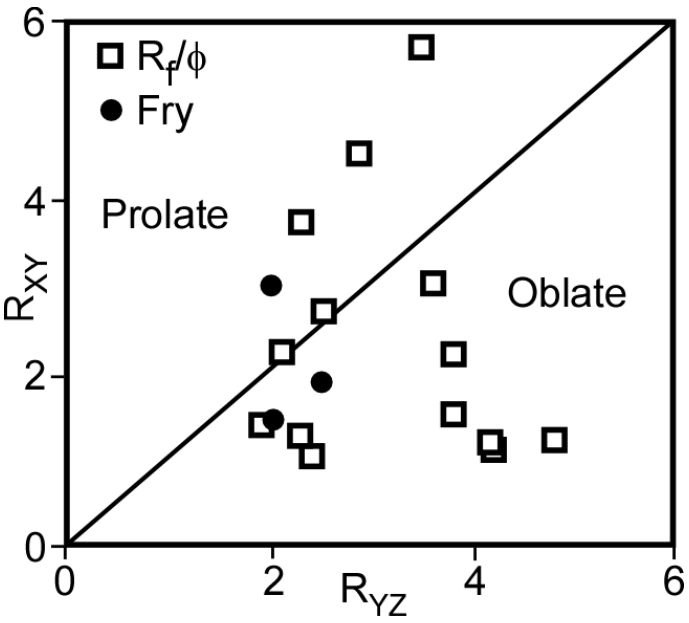

Flinn diagram showing the strain symmetry as obtained by Rf/ϕ (white squares) and Fry (black triangles) analysis. Rf/ϕ and Fry data from the same sample are connected by dashed tie lines.

Christine Kumerics also analysed vein sets in fifteen outcrop surfaces, thirteen in metapelite of the Ikaria nappe and two in phyllite of the Messaria nappe for determining the degree of rotation during extensional shearing. The degree of rotation is expressed by the so-called kinematic vorticity number, Wm. Wm=1 means that the degree of rotation equals the degree of stretching and the shear zone would not shorten perpendicular to its walls during shearing, i.e. shearing is by simple shear. Wm=0 indicates no shear-related rotation at all and the deformation would be described as pure shear. The distribution of the deformed veins is consistent with top-to-the-NNE shear. Wm ranges from 0.1 to 0.7 and Rf from 1.8 to 8.9. In general, Rf agrees with values of 2.4 to 19.9 for RXZ of finite-strain analysis and again demonstrates heterogeneous shortening perpendicular to the shear zone.

Geochronology

For constraining the age of mylonitic shearing in the Messaria shear zone and also the speed at which the Messaria extensional system slipped, we carried out Rb/Sr, 40Ar/39Ar, fission track and (U-Th)/He dating in the footwall of the Messaria extensional fault system. The data are not given here but can be found in Kumerics et al. (2005). Some of the sample localities will be described in the field trip section below.

Rb/Sr data

Both analyzed samples are from the uppermost Ikaria nappe within the Messaria shear zone and they both are characterized by isotopic disequilibria. Detailed thin-section investigation of the quartzitic schist (sample IK99XD) suggests complete synkinematic recrystallisation; however, internal isotopic equilibrium on the mineral scale has not been achieved. On an isochron plot, the data only allow calculation of a loosely defined reference line corresponding to an age of 12.9±3.5 Ma (2σ errors). As no alteration features are observed, disequilibria are likely to correspond to preservation of isotopic relics. The age value is therefore interpreted as a maximum age for the last stages of mylonitisation.

The mylonitic metapegmatite sample IK02-4 shows severe Sr-isotopic disequilibria even for extremely deformed domains. For all analyzed white mica fractions, apparent ages have been calculated using the isotopic signature of apatite for reference. There is a clear correlation between sieve fraction (as a proxy for grain size) and apparent age for white mica separates. While the apparent age of 58±1 Ma for the 250-160 µm sieve fraction can be interpreted as a maximum age for deformation, the apparent age of 375±6 Ma for the 500-355 µm fraction points to only limited Sr isotope exchange among dynamically recrystallising phases and/or to presence of ground, but not recrystallised primary pegmatitic white mica. The apparent ages for slightly bent and kinked mica fish inner domains of 417±6 and 458±7 Ma are 'mixed' ages as well, without direct geological meaning. However, the oldest age of 458±7 Ma is a minimum age for protolith crystallization.

The latter age is poorly defined but strongly suggests to us that the magmatic event hat produced the pegmatite of the Ikaria nappe does actually belong to the Pan-African magmatic activity that is typical for parts of the Menderes nappes of adjacent western Turkey and underpins our tentative correlative of the Ikaria nappe to the Menderes nappes.

40Ar/39Ar data

Mylonite: White mica from a mylonitic metapegmatite (IK02-4) and a metasediment (IK02-8) sample were dated with the spot-ablation technique. Both samples are intensely foliated and the foliation is made up by quartz, opaques

and phengite, which is sheared and recrystallised in distinct foliation-parallel shear zones. The sections for 40Ar/39Ar dating are from the most thoroughly sheared and recrystallised parts of the samples.

In each section between 6 and 10 spots were analysed. The ages of IK02-4 range from 13.8±4.8 to 5.4±1.8 Ma and have a weighted mean age of 10.8±1.1 Ma (2σ errors). The ages from IK02-8 range from 11.1±0.3 to 9.5±0.5 Ma and show a weighted mean age of 10.5±2.4 Ma. We interpret the ages to date phengite recrystallisation during ductile deformation in the Messaria shear zone.

Altherr et al. (1982) reported K/Ar and Rb/Sr white mica ages of 11-10 Ma from metasediments in the footwall of the Messaria extensional fault system. Our detailed thin-section work on samples from localities where Altherr et al. (1982) collected their samples suggests that white mica completely recrystallised during mylonitisation. Therefore, we argue that mylonitisation and recrystallisation caused complete isotopic re-equilibration and that the K/Ar ages date mylonitisation-related mineral growth. The ages of Altherr et al. (1982) and our ages all young in a northward direction.

Granites:

Muscovite and biotite crystals from granite samples IK1, IK2 and IK7 were analysed with the step-heating laser-probe technique. IK1 and IK2 are from the I-type Raches granite and IK7 from the S-type Xylosirtis granite. Biotite from sample IK2 yields a plateau age of 17.9±0.5 Ma (2σ errors) for 90% of released argon. Biotite from sample IK7 gives a plateau age of 10.7±0.3 Ma for ~81% of released argon, and muscovite from the same sample yields a slightly younger but within error similar plateau age of 10.2±0.5 Ma for ~100% of released argon. Biotite from sample IK1 gives an age of 9.3±0.9 Ma; however, because biotite was too small to provide a complete age spectrum this age is based on one single heating step only.

The 17.9 Ma biotite 40Ar/39Ar age from sample IK2 of the I-type Raches granite is much older than all other ages from this granite and its U-Pb zircon age (see below) and thus poorly understood.

Low-temperature thermochronology

The zircon fission track ages from the footwall of the Messaria extensional fault system range from 10.3±0.3 Ma in the south to 6.3±0.3 Ma in the north (2σ errors). The apatite fission track ages are between 8.4±0.8 Ma (south) and 5.2±0.9 (north) and the apatite (U-Th)/He ages range from 6.0±0.3 Ma (south) to 3.6±0.2 (north). All ages consistently young in a northward direction.

The samples from the hangingwall of the Messaria extensional fault system yielded no apatite and zircon. Fission track ages form the Ampelos nappe of Samos, which is correlative with the Messaria nappe in the hangingwall of the Messaria extensional fault system, range from 20-18 Ma (Kumerics et al. 2005; see Ring et al. for Samos in this volume).

Preliminary U-Pb zircon ages from the various granites

We analysed zircons from sample IK2 from the I-Type Raches granite, from sample IK-05/7 from the S-type Karkinagrion granite and sample IK7 from the S-type Xylosirtis granite by excimer laser ablation (ELA-ICP-MS) at the Research School of Earth Sciences in Canberra, Australia. When combined these cores and rims yield the following pooled 206*Pb/238U ages: 13.8±0.3 Ma (N=31, MSWD=8.3) fro sample IK-2, 13.6±0.4 Ma (N=15, MSWD=5.1) for sample IK-05/7 and

14.2±0.3 Ma (N=9, MSWD=2.8) for sample IK7. All ages overlap with 2σ error. The ages became available just before this field trip guide was submitted and will thus no be discussed further.

Tectonic significance of geochronological results

Cooling of the footwall of the Messaria extensional fault system

Temperature-time (T-t) paths for the I-type Raches granite (IK1 from Armenisits and IK2 from the south coast west of Karkinagrion), the S-type Xylosirtis granite (IK7) and the metasediments (IK6) in the footwall of the Messaria extensional fault system are slightly different (Figure 19). They indicate rapid cooling from ~700°C to <100°C within <9 Ma. Sample IK1 from the I-type Raches granite yields the most rapid cooling rate of >100°C between 9.3 Ma and 6.7 Ma followed by slow cooling thereafter. Sample IK2 depicts a similar shape of the cooling curve but cooling of this sample occurred ~2 Myr earlier than that of sample IK1. IK2 shows a fairly steady cooling from its intrusion temperature to about the apatite partial annealing zone. Sample IK7 from the S-type Xylosirtis granite had a slightly different cooling history with average cooling rates

of ~80°C Myr-1 between ~10 Ma to ~5 Ma. Metasediment sample IK6 cooled somewhat slower at rates of ~70-75°C Myr-1 between ~10 Ma to ~5 Ma (Figure 19). The mean track lengths of apatite range from 14.14±0.16 m to 14.18±0.12 m for the I-type Raches granite, 14.43±0.21 m to 14.51 ± 0.19 m for the metasediments, and 14.19±0.36 m for the S-type granite and support rapid cooling.

Figure 19. T-t diagram

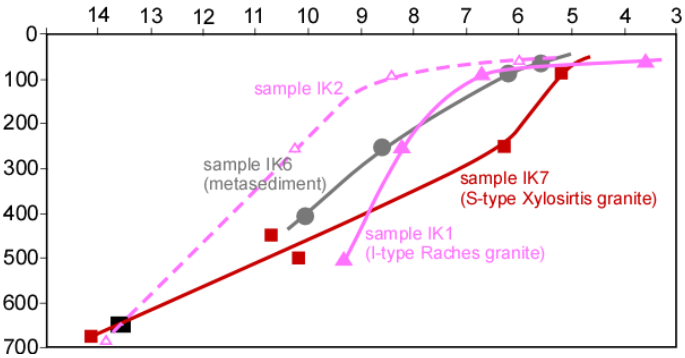

T-t diagram showing cooling of metasediment sample IK6, sample IK7 from the S-type granite and sample IK1 from the I-type granite in footwall of the Messaria extensional fault system (note that intrusion age for sample IK2 of I-type Raches granite has been plotted as well). The white mica K/Ar age from sample I45/4 (Altherr et al. 1982), which is from a locality close to that of IK6 (Figure 2), has been used to extrapolate the path for IK6 to higher temperatures. Because the K/Ar white mica age of I45/4 reflects mica growth during mylonitization, a temperature range of 350-450°C has been attributed to this K/Ar age. Muscovite and biotite from the two granites show no evidence of deformation or fluid-related alteration, therefore we infer that the 40Ar/39Ar ages of these minerals reflect cooling below temperatures of 450 ± 50°C (biotite) and 500 ± 50°C (Villa 1998) (see Kumerics et al. 2005 for similar figure with temperature range for various dated minerals). The T-t path for the I-type granite is steeper for the interval between ~9-7 Ma than the paths for metasediment sample IK6 and sample IK7 from the S-type granite.

We envisage that the T-t path for the metasediments of the Ikaria nappe reflects extension-related cooling during and after greenschist-facies metamorphism and that the relatively constant cooling rate is controlled by a relatively constant rate of extensional slip. The small S-type Xylosirtis granite intruded relatively deep during extensional faulting and cooled together with the surrounding metasediments. The generally slightly faster cooling history of the large I-type Raches granite may reflect intrusion into higher crustal levels than the S-type granite. More interesting are the two cooling curves of the two samples from the Raches granite. The similar shape of both curves seems to indicate that steady cooling was controlled by relatively steady motion on the Messaria extensional fault system. Unfortunately we do not have a U-Pb age for sample IK1 from the north coast. If one projected the curve for IK2 down to higher temperatures then it seems that the intrusion age for IK1 would be ~2 Myr than that for IK2. Alternatively, IK1 has a similar intrusion age than IK2 but this part of the granite cooled relatively slowly between ~13.5-9 Ma and became only at ~9 Ma been caught up in the shear zone.

Slip rate for Messaria extensional fault system

Kumerics et al. (2005) showed that the decrease of the zircon and apatite fission track and apatite (U-Th)/He ages in a direction parallel to hangingwall transport on the Messaria extensional fault system reflects the progressive southward migration of footwall exhumation. The decreasing ages are related to the lateral passage of subhorizontal isotherms at the top of the footwall. Hence, the data can be used to estimate apparent slip rates for the Messaria extensional fault system from the inverse slope of mineral age with distance in the slip direction.

Samples IK1 - IK4 from the I-type Raches granite in the western part of the island were taken from a NNE-SSW pofile parallel to the slip direction on the Messaria extensional system and yield apparent slip rates of 6.0±0.9 km Myr-1 (apatite (U-Th)/He), 8.4±6.0 km Myr-1 (apatite fission track) and 9.7±2.8 km Myr-1 (zircon fission track).

We also calculated an apparent slip rate from the K/Ar white mica ages of Altherr et al. (1982) from the Messaria shear zone. The fact that the K/Ar white mica ages of Altherr et al. (1982) consistently young in a northerly direction and are consistently slightly older than the zircon fission track ages supports the interpretation that the white mica ages date white mica recrystallisation during ductile deformation in the Messaria shear zone. This interpretation is in line with our Rb/Sr age of 12.9±3.5 Ma for sample IK99XD, which is a maximum age for mylonitisation, and our 40Ar/39Ar data of 10.8±1.1 Ma (sample IK02-4) and 10.5±2.4 Ma (sample IK02-8). The white mica ages of Altherr et al. (1982) yield an apparent slip rate of 7.3±1.0 km Myr-1, which is similar to the apparent slip rates obtained from low-temperature thermochronology.

Average apparent slip rates at the Messaria extensional fault system were ~6-9 km Myr-1. This rate would yield a displacement of ~70-100 km for the period from ~14-3 Ma.

Summary and discussion

A low-angle ductile shear zone associated with two brittle detachment faults of Late Miocene to Pliocene age has been mapped on Ikaria Island. The ductile shear zone formed in the uppermost ductile crust under mid-greenschist facies conditions. Ductile shearing was not by simple shear and involved a component of vertical shortening. Cooling in the footwall of the extensional fault system was rapid and the offset was of the order of 70 km or even more. The dominant shear sense was top-to-the-NNE; during footwall unloading and doming of the extensional fault system minor late-stage antithetic shears developed.

Extensional structures on Ikaria

The progressive superposition of ductile, ductile-brittle and brittle structures in the footwall of the Messaria extensional fault system, brittle deformation in the hangingwall and the decrease of cooling ages parallel to the northward slip direction of the hangingwall reflects progressive southward migration of footwall exhumation and is typical for extensional fault systems above metamorphic core complexes.

Initial movement in the ductile Messaria shear zone of the Messaria extensional fault system at ~14 Ma was accompanied and aided by the intrusion of synkinematic granites (Figure 20a) and a relatively high thermal field gradient of ~30°C km-1. The Messaria extensional fault system operated from ~350-400°C to at least 80°C between ~14-3 Ma. Because biotite in samples from the northern portion of the shear zone was stable during mylonitisation, temperatures were slightly higher than 400°C in the northern part of Ikaria. T-t paths indicate rapid cooling as the footwall was exhumed to the surface. The Messaria detachment probably rooted at the brittle/ductile transition and the Messaria shear zone in the underlying ductile crust (Figure 20a). The fact that the cooling rates of both the S-type Xylosirtis granite and the metapelite of the Ikaria nappe are largely similar is thought to be due to a relatively deep intrusion of the small granite during extensional shearing and that both rocks units were then exhumed and cooled together. The steeper cooling curve for the large I-type Raches granite is interpreted to reflect intrusion into higher crustal levels but according to the zircon ages concurrently with the intrusion of the S-type Xylosirtis granite at ~14 Ma.

Figure 20. Three stage evolution

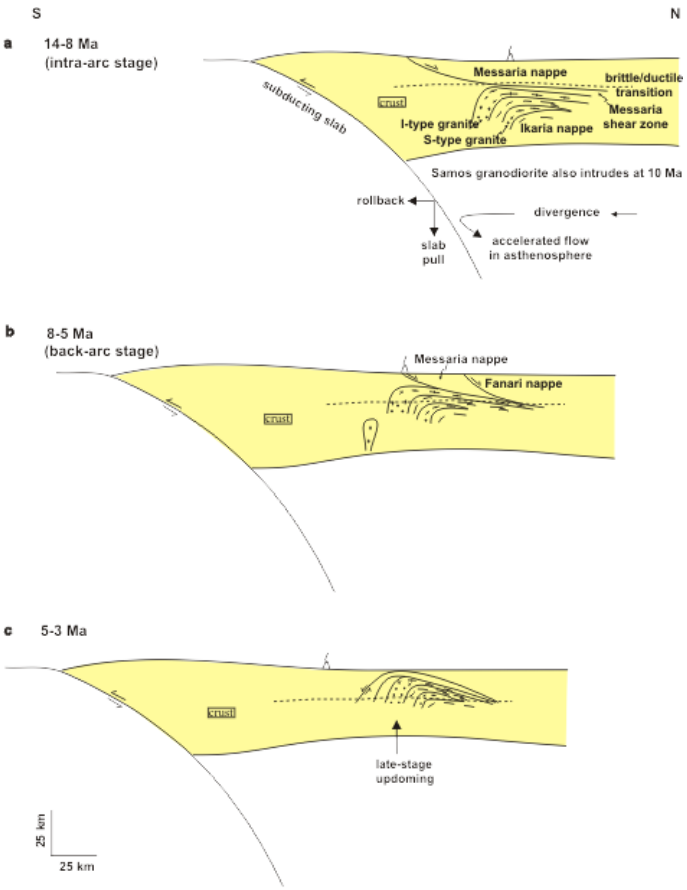

Three stage evolution of extensional deformation on Ikaria. (a) The inception of Messaria extensional fault system was aided by the intrusion of the S-type granite and later also by the intrusion of the large I-type granits in the magmatic arc of the Hellenic subduction zone. Note that the ~10 Ma old granodiorite and the 11 Ma old volcanic rocks on Samos Island (Weidmann et al., 1984) are of the same age. We envisage that subduction-zone retreat caused intra-arc extension at this stage. The simplified arrows show accelerated corner flow in the asthenosphere behind the retreating subduction zone, which caused relative plate divergence in the intra- and back-arc area. Asthenospheric flow in the arc and back-arc region behind retreating slabs is forced to accelerate in the horizontal to fill the free space caused by the retreating subduction zone causing plate divergence. (b) The Messaria shear zone moved into brittle crust and is juxtaposed with Messaria detachment. The magmatic arc probably shifted southward. (c) Late-stage updoming of the footwall as a response to unloading.

Average slip rates at the Messaria extensional fault system were ~6-9 km Myr-1 and imply a displacement of ~>70 km. This displacement and the maximum depth of 15 km for the onset of extensional faulting yields a dip angle of ~15°, or even less, for the Messaria extensional fault

system. A prerequisite for the development of low-angle faults appears to be that they have to reactivate earlier fault planes. Pre-extension thrusts were not observed on Ikaria. However, the occurrence of the high-pressure Messaria nappe above the non-high-pressure rocks of the Ikaria nappe suggests that the contact between these two nappes was a thrust, probably the Cyclades-Menderes thrust. If so, extensional reactivation of this thrust plane would be in line with the low-angle nature of the Messaria extensional fault system.

How does the Fanari detachment relate to the Messaria extensional fault system? The occurrence of allochtonous Pliocene sediments in the hangingwall of the Fanari detachment indicates that movement on it continued until or commenced after ~5 Ma. Because movement on the Messaria extensional fault system lasted until ~3 Ma, it appears feasible to assume that the Fanari detachment is a brittle fault in the hangingwall of Messaria extensional fault system and hence is ultimately related to the latter (Figure 20b).

The kinematic indicators in the Messaria shear zone and the brittle Messaria and Fanari detachments together with the spatial trend of footwall cooling ages indicates a general top-to-the-NNE sense of movement. We envisage that the late-stage top-to-the-SSW shear-sense indicators reflect minor antithetic extensional structures related to footwall unloading and updoming of Ikaria (Figure 20c).

Comparisons with extensional fault systems on Samos Island

Because most of the Aegean region is under water any regional correlations are necessarily speculative. Scaling relationship for faults suggests that large-scale structures such as the Messaria extensional fault system must continue laterally over great distances as far as Samos Island (Figure 3). For us a correlation of the Fanari and Kallithea detachments with the Messaria extensional fault systems appears to be reasonable. Both detachments have the same shear sense and have non-metamorphic units in their hangingwall, which contain Pliocene sediments. Inception of the Kallithea detachment is fairly well dated at ~10 Ma age (Ring et al. 1999b) and a granodiorite dike in its footwall yielded a zircon fission track age of 7.3±0.6 Ma (Sa7) (Ring et al. this volume). If it was accepted that the Fanari detachment is related to the Messaria extensional fault system, then the Kallithea detachment would also be part of the Messaria extensional fault system.

Ductile extensional shearing on Samos has no relationship to the brittle Kallithea detachment. One zircon fission track age of 14.1±0.8 Ma (Sa9) (Ring et al. this volume) from the Basal unit suggests that the Kerketas extensional system is slightly older than the Messaria extensional fault system on Ikaria. Ductile extension and exhumation of the Ampelos nappe below the Selçuk extensional system lasted until in the Early Miocene as indicated by zircon fission track ages of 20-18 Ma (see above), which consistently young northeastward in the direction of hangingwall slip. The zircon fission track ages indicate that the Selçuk and Kerketas extensional systems are unrelated to each other and also show that both extensional systems are unrelated to the Messaria extensional fault system.

Field trips

Figure 21. main roads on Ikaria

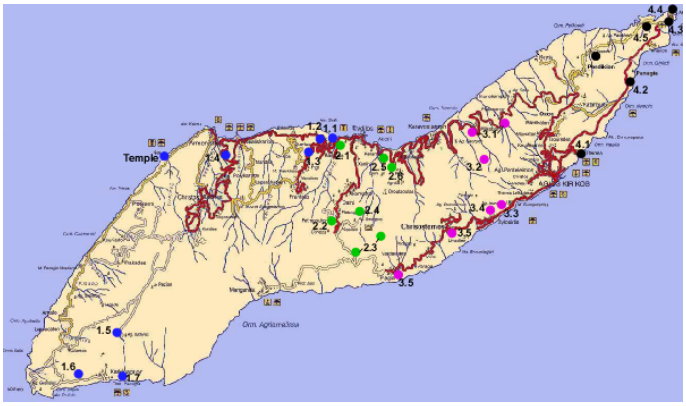

Roadmap showing main roads on Ikaria and field trip stops.

The map shown in (Figure 21) shows the main road on Ikaria and also the field trip stops.

Day 1: Archaeological Museum and the I-type Raches granite

Kampos, the old capital of Ikaria is a good place to start a field trip. Leave the ferry from Piraeus in Evdilos and drive about 5 km to the west. Stay at Dionysos Rooms (http://www.island-ikaria.com/hotels/dionysos.asp), Vassilis, the owner, is a very nice and entertaining bloke who is used to weird geologists. He is also the curator of the archaeological museum (Stop #1.1). Stroll down to the beach in phyllite of the Messaria nappe and find ductile to brittle-ductile top-NNE shear bands in the road cut on the left hand side as you walk down to the beach.

The I-type Raches granite is generally believed to be ~22 Ma old. This inference is based on a Rb/Sr whole-rock errorchron published by Altherr et al. (1982). Faure et al. (1991) and Kumerics et al. (2005) showed that the granite is synkinematic to top-NNE extensional shearing and mylonite dating and rapid footwall cooling indicate that extensional shearing did not start before ~12-11 Ma. Our dating of magmatic zircons form the I-type Raches granite and the smaller S-type Karkinagrion and Xylosirtis granites yielded intrusion ages of ~14-13 Ma (see above).

Stop #1.1: Archaeological Museum in Kampos

Situated on a hill, which was the ancient citadel of Oenoe, the first capital of Ikaria, the Kampos Archeological Museum contains over 250 finds from Ikaria. Museum items include Neolithic tools, pottery vessels, clay statuettes, columns, coins, and carved headstones. The museum is located within a courtyard that also contains the Church of St. Irene, built on the site of an ancient temple to Dionysus. Usually open three times per week from 10:00am to 3:00pm, but Vassilis would open it for you almost any time.

Stop #1.2: Extensional structures in phyllite of Messaria nappe

Drive from Kampos towards Armenistis, about where the last houses of Kampos are close to the turnoff to Fratato there are greyish to black phyllites exposed in the roadcuts with nice brittle to brittle-ductile shear bands and normal faults indicating top-NNE shear (Figure 22).

Figure 22. top-N shear bands

Photograph showing various sets of top-N shear bands in metapelite of the Messaria nappe. The shear bands in the upper part of the photograph have a low-angle geometry. The shear bands in the lower half of the photographs have steeper angles and are distinctly more brittle-ductile in nature and grade into normal faultss.

Stop #1.3: Road to Fratato; folded granite and phyllite sequence

Drive uphill on the road to Fratato. To the west you see outcropping Raches granite and to the east below the road are rocks of the Messaria nappe. Granite occurs as dikes and lenses in phyllite of the Messaria nappe and both rocks are tight to isoclinally folded. Mapping at the 1:10,000 scale in 1999 by 3rd and 4th year students suggests that this granite is the I-type Raches granite (Figure 23). Regional structural analysis shows that folding and stretching of the granite and its country rock is related to top-NNE extensional shearing. This in turn shows that the Raches granite is also deformed together with the hangingwall plate of the Messaria extensional fault system. We have found no field evidence for intrusion of the I-type Raches granite into the rocks of the Messaria nappe. In line with Lister & Davis (1989) we envisage that large relative displacement along the Messaria detachment caused locally complex excisement geometries when the detachments cut into the upper plate thereby juxtaposing lower and upper plate rocks causing them to deform together. The Fanari detachment can

be envisaged as a late excisement splay that cut into the upper plate allowing the active detachment to rise through the section.

Figure 23. Messaria nappe S of Evdilos

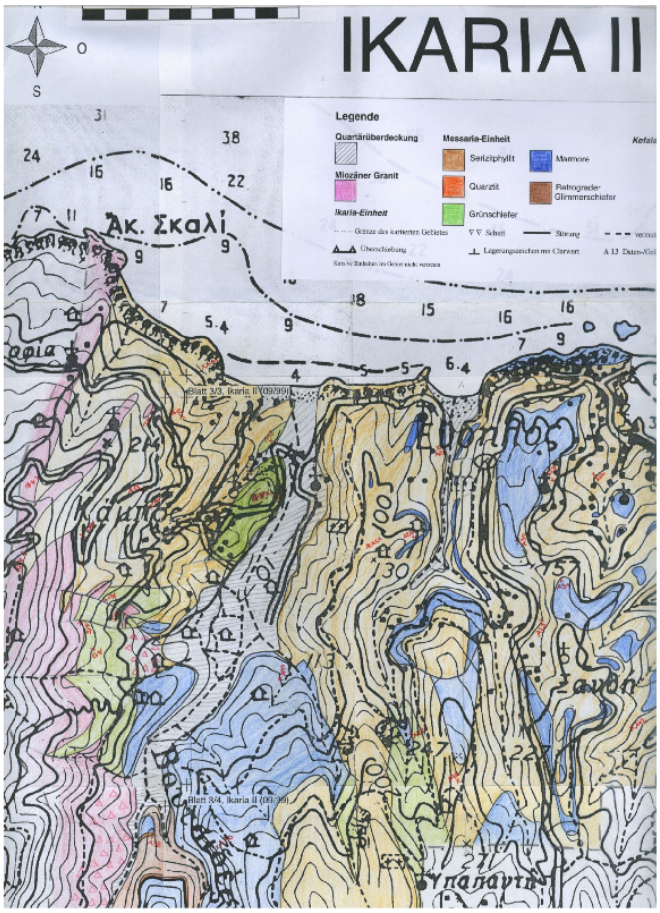

Geologic map at 1:10,000 scale of the Messaria nappe S of Evdilos. The Raches granite in the W is shown by the pink colour; the granite is folded with the sericite phyllite (shown in light brown) and also occurs as lenses in the Messaria nappe. Also shown is the relatively large greenschist body in Kampos.

Turn round and go back to the Evdilos-Armenistis road and drive to Armenistis. Most of the drive is in variably deformed Raches granite. Near Armenistis there are two nice sandy beaches. Usually beaches in the Cyclades are rather rocky but granite weathering gave rise to these fairly rare sandy beaches.

Stop #1.4: Ultramylonitic granite S of Armenistis

Just when you come into Armenistis there is a turnoff to the S (left up the hill) to Christos Raches. The road climbs up in hairpin turns and after about 1-1.5 km there is a sharp right-hand turn followed by a left-hand one. After the latter there are extremely deformed granites exposed in the roadcut to your left. The rock is very weathered but the very fine grain size and the ultramylonitic deformation of the granite is ubiquitous (Figure 24). Except the extremely narrowly spaced foliation and numerous late joints there are hardly any structures visible. However, occasionally you will find very nice small-scale shear bands (a hand lense comes in handy for this exercise). The Messaria shear zone dips at about 10-20º to the N and it is likely that the outcrops are very close to the detachment above your heads.

Figure 24. ultramylonitically deformed Raches granite

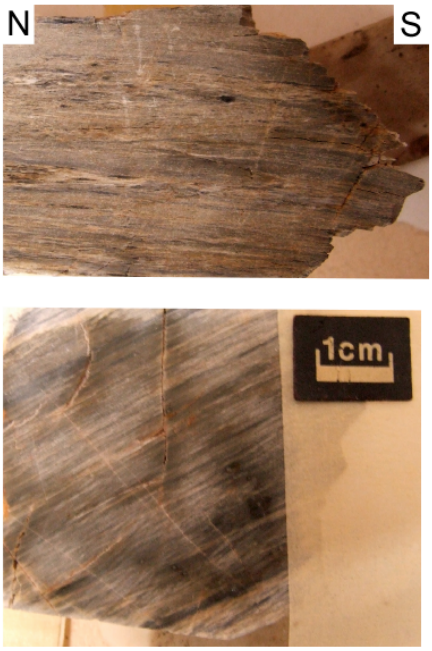

Photographs of ultramylonitically deformed Raches granite.

Head towards Christos Raches and then try to find the right road to the dams and Agios Isodoros by bearing right in Christos Raches. (The pedestrian area in the village is worth a wander.)

Stop #1.5: Deformed Raches granite near Agios Isodoros

After passing the dams the dirt road heads to the SW and is more or less flat. At the turnoff bear left and the road slightly climbs up to a ridge in front of you. On the ridge, the deformed granite in the Messaria shear zone dips almost

horizontally. You reached the main crest of the island and here the shear zone has a subhorizontal attitude (Figure 7). The granite has a well developed foliation and NNE trending stretching

A bit down the hill is the monastery of Agios Isodoros. Have a look down to the south: to the right (west) you see more whitish I-type granite. To the left (southeast), the outcrops have a more yellowish-brownish colour suggesting a difference in granite composition (see stop #1.7).

Drive back down to the turnoff and then take a left. The road goes in Raches granite and winds down to west where it eventually hits the road from Armenistis to Karkinagrion. Take another left at the turnoff; the road to Karkinagrion all of a sudden turns into a wide asphalt road.

Stop #1.6: Raches granite west of Karkinagrion

When the road descends in wide bends east towards Karkinagrion the Raches granite is hardly deformed at all and exhibits typical granite textures. There are some rather large potassium feldspar minerals in a quartz-plagioclase matrix; biotite is usually abundant. Sphene, red allanite, apatite, titanomagnetite, zircon and tourmaline occur as accessory phases. It is from this area were sample IK7 was collected.

Stop #1.7: Relationships between the Raches and Karkinagrion granites east of Karkinagrion

Drive through Karkinagrion to the east. On the western side of a N-S running creek the I-type Raches granite is exposed, whereas on the eastern side of the creek a yellowish to brownish two-mica granite with abundant white mica is exposed and we refer to this granite as the S-type Karkinagrion granite. Both granites exhibit magmatic textures and hardly any signs of tectonic deformation. The Karkinagrion granite contains occasionally garnet and also tourmaline. There is a faint steeply-dipping N-S-striking foliation visible in the Karkinagrion granite. In a few places fabrics suggest that the S-type Karkinagrion granite intruded the I-type Raches granite. However, as shown above the intrusion ages for both granites overlap within 2σ error. Sample IK-05/7 was collected in this area. There are also late-stage garnet- and tourmaline-bearing aplite dikes that crosscut both granites.

You could go back to Kampos along the north coast and visit the temple of the Ikarian Artemis in Nas. The road is winding and not in good conditions but the scenery and the temple is worth to take the coastal road. The drive is in variably deformed Raches granite, which in part shows spectacular shear bands (Figure 25).

Figure 25. Raches granite

Raches granite showing top-NNE shear bands, road at the NW coast towards Nas.

During the 6th century BC the Ikarians built a temple in Nas to honour the mother goddess Artemis, patroness of sailors and protector of hunters and wild animals. Nas was probably the first settled area of Ikaria and throughout antiquity its safe anchorage was an important staging point on the sailing route from Asia Minor to Delos, especially during the months of October and November, season of the Apatouria in ancient times, when, due to the strong southeastern winds, voyagers to Delos preferred to sail along the north coast of Ikaria, where they would get supplies and shelter from bad weather. Nas never developed into a town in the ancient meaning of the term. The people who lived here lived on the goods the sea gave them, on bird and deer hunting and bred their own animals. Nas is known for the temple of Tavropolos Artemis (tavropolos means 'herd of bulls'). The temple of Tavropolio must have been a late Minoan structure as the goddess was worshipped in the late Minoan period. Ikaria was one of the first stops of Artemis from Asia Minor and Tavropolio a shrine celebrated throughout Greece. Tavropolio prospered in the years when worship of the goddess was at its peak in the era of Attic civilization. According to the historian Ioannis Melas, Tavropolio was probably not only the temple of the goddess Artemis but also a settlement, one of the four ancient settlements on Ikaria, but no evidence has come to light to prove it. It is also very possible that there is a relationship between the temple of Nas and the other temples of Artemis that existed in that section of the Aegean Sea – Samos, Fokea, Chios, Patmos, Delos and Efessos. Around 1830 local Ikarian villagers melted down most of the

temple's stone blocks in order to build a church. Legend has it that the ancient temple's statue of Artemis is buried somewhere in the river. Snorkeling just off the coast one can see the massive columns of the temple. The pier of the ancient port and the floor of the sanctuary still survive. A few kilometres away from Nas is Cape Kavo Papas. 'Papa' was one of the older names of the god Attis, the manifestation of Mother God (whom the Greeks would later identify as the goddess Artemis).

In 1938 the famous Greek archaeologist Leon Politis came to Ikaria to take over the first archaeological excavation of Nas. Although well known, the temple was not a large building. Politis started his search 25 m west of the river, near the lime kiln of the 19th century and realised that the dimensions of the temple were 9.70 x 3.75 m. It was founded on an enhanced basis, which was necessary on this unstable, sloping ground. The second building, 10 m to the south, was smaller (3.10 x 2.15 m) and probably sheltered the famous wooden statue of the goddess. Among other objects, he found an elaborated wine cup from Rhodes, showing a chamois, a buckle with a lion head, a beautiful statue head of the Hellenistic years, as well as two bodies from women's statues, one of them from the 5th century and the other from the 2nd century BC. Politis also revealed some fulcrums of ionic and doric columns and saw pieces of columns in the sea.

Day 2: Messaria shear zone in the central part of the island

Stop 2.1: Greenschist

Take a left towards Evdilos at the main road and go downhill for about 400m. On your left-hand side there is deformed greenschist of the Messaria nappe exposed. The greenschist exhibits the typical subhorizontal extension-related foliation and a well-expressed NNE-plunging stretching lineation. Have a good look around and find kinematic indicators which will give a top-NNE shear sense.

A bit further down the road are ruins of a 1st century AD Byzantine odeon (Figure 26), which served as a central meeting place and forum for musical and theatrical events for the people of the ancient Ikarian capital Oenoe. Oenoe was a prosperous city known throughout the ancient world for its viticulture.

Figure 26. Byzantine Odeon in Kampos

The 1st century AD Byzantine Odeon in Kampos.

Stop 2.2: Domino-style tilting in upper plate

Take the turnoff to Dafni in Evdilos and drive for about 5-6 km uphill to the south. You go through phyllite and marble of the Messaria nappe. South of Dafni the road drops down a bit into a N-S oriented gorge and in the cliff on the right-hand side some metre-scale tilted marble blocks can be seen (Figure 27). The blocks are back-tilted to the S and are separated from each other by N-dipping small-scale faults.

Figure 27. Tilted marble blocks

Tilted marble blocks in the Messaria nappe.

Stop 2.3: Base of Messaria nappe

Drive on to the south and climb up on the road to the crest of the island. There you will find a little church on the left-hand side of the road in a thick marble sequence. From the church or the hill just above it you have a good view down to the north overlooking the rugged morphology of the Messaria plain (basically made up by phyllite and marble of the Messaria nappe). The topography to the east in the monotonous metapelite of the Ikaria nappe is quite different, as is the topography in the granite to the west. Our interpretation is that the upper plate of the Messaria extensional fault system, the Messaria nappe in the central part of Ikaria, is cut by a number of brittle faults and only a few of them also affect the lower-plate rocks. Also note that to the north the slopes dip rather shallowly to the N, whereas to the S the slopes are steep giving the island its overall asymmetric architecture.

The road drops down to the south and makes a turn to the east. You see the base of the marble, which is the base of the Messaria nappe, exposed in the road cut. The contact is not spectacular. The marble is strongly brecciated (Figure 28) and the underlying metapelite shows brittle-ductile deformation and late upright folding.

Figure 28. Brecciated base of Messaria nappe

Brecciated base of Messaria nappe at road from Evdilos to the south coast. Composite photograph on top shows road section; photograph on left show pronounced brecciation of marble; photograph on right depicts upright folding of metapelite below the brecciated marble.

Mylonite sample IK99XD described above was collected ~1-2 km ENE from the church at the pass. Walk along the crest line (Figure 29) across marble with abundant karst features (Figure 30) and you will find occasional patches of rather whitish and strongly deformed quartzite below the marble. This quartzite forms lenses at the boundary between the Messaria and Ikaria nappes. This boundary is commonly decorated by brownish, in part dolomitic marble (Figure 31). Towards the ENE the crest line slightly climbs up and WSW of the highest knoll (909 m.a.s.l.) you will find whitish quartzite below whitish marble. The marble tends to become impure towards its base and contains white mica and other minerals. In quartzite sample IK99-31 chloritoid is in equilibrium with kyanite, andalusite and chlorite. Kyanite also occurs as inclusions in chloritoid. The sample is characterised by the lack of biotite. The occurrence of kyanite and andalusite in equilibrium in IK99-31 from the Ikaria shear zone constrains pressures at 3-4 kbar. The presence of chloritoid with chlorite-aluminosilicate and the lack of biotite suggest temperatures of 350-400°C (Figure 32c, d). Our interpretation is that the P-T data reflect the physical conditions during mylonitisation in the Messaria shear zone and indicate a thermal field gradient of 25-35°C km-1 during movement in the Messaria shear zone. The intrusion of the synkinematic granites are in line with an elevated geotherm.

Figure 29. Steep marble cliff

Steep marble cliff. Base of the cliff marks the boundary between Messaria and Ikaria nappe.

Figure 30. Foliation planes in Messaria marble

Foliation planes in Messaria marble showing abundant karst features. The karst developed along joint surfaces.

Figure 31. Base of Messaria marble

Base of Messaria marble is decorated by 1-2 m thick brownish marble horizon.

Figure 32. Microphotographs of samples

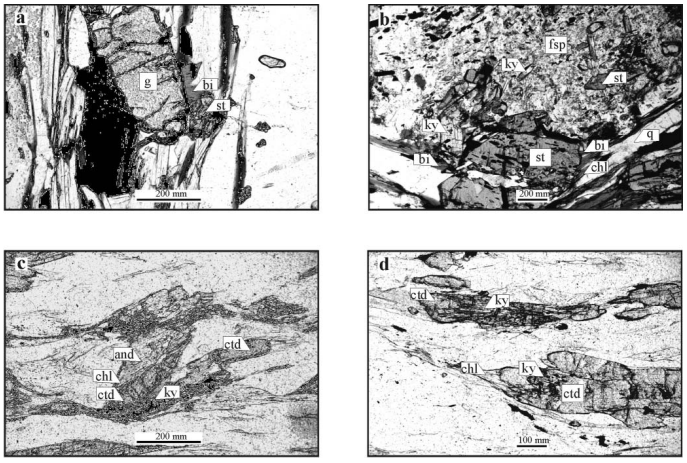

Microphotographs of samples from the Ikaria nappe and the Messaria shear zone. (a) Staurolite, chlorite and muscovite in equilibrium with biotite and garnet, sample IK02-6a. (b) Sample IK02-16 showing chlorite-staurolite-biotite-kyanite paragenesis; staurolite is in equilibrium with plagioclase and biotite, or occurs as an inclusion in plagioclase; kyanite occurs as an inclusion in plagioclase, or in equilibrium with staurolite, plagioclase and biotite; chlorite is in equilibrium with biotite and staurolite in matrix. (c) Chloritoid in equilibrium with kyanite, chlorite and andalusite in sample IK99-31. (d) Kyanite inclusions in chloritoid; sample IK99-31.

Stop 2.4: Koskina Castle and marble of the Kefala klippe

Drive back towards Evdilos and after ~2 km an unpaved road branches off from the main road to the southeast. Follow that road until the very end, from there here is a footpath to the Castle of Koskina, which is an 11th century A.D. Byzantine fortress located on a mountain peak overlooking the village of Koskina in the center of Ikaria (Figure 33). The Ikarians built the fortress because the Byzantine empire cut back its naval defense and the Aegean became open to inroads from pirates and Italian adventures. Some pirates fleeing Patmos arrived in Ikaria and where executed by the local population. Inside the castle is the church of St. George Dorganas.

Figure 33. Messaria nappe and the Kefala klippe

Photograph showing the Messaria nappe and the Kefala klippe with the castle of Koskinon. Note the gentle dip to the N; view is to the E.

The fortress is built on marble of the Kefala klippe. There is a hornblende diorite dike exposed at the northern end of the klippe. The diorite is usually severely hydrothermally altered and pumpellyite, clinozoisite and sericite replaced magmatic plagioclase, and actinolite, chlorite, titanite and prehnite replaced brown hornblende. However, in rare cases fresh plagioclase and brown hornblende survived. Altherr et al. (1994) reported scattering K-Ar hornblende ages of 67 to 80 Ma from those diorites. One single amphibolite, which is intercalated within the marbles, also yielded a Late Cretaceous K-Ar hornblende age of 84 Ma. The host marble is supposed to be Late Triassic in age (Altherr et al. 1994).

Drive back to Evdilos and then turn right and follow the main coastal road to the east.

Stop 2.5: Extensional structures in upper Ikaria nappe

For the first ~2 km east of Evdilos you are still driving in phyllite with intercalated marble of the Messaria nappe. The contact to the underlying Ikaria nappe is generally poorly exposed and strongly overprinted by brittle faulting. About 800 m east of Evdilos in the first major bend in the road just S of the headland of Arethoussa, there a brownish-white marbles and phyllites which are heavily cataclasised. If you walk across the road and go down to the cliff you will be below the detachment and will find ductile top-NNE shear bands.

There are numerous outcrops in the roadcut on the right-hand side of the road of deformed quartz and pegmatite veins (Figure 14), (Figure 34). Most of the veins are parallel to the foliation and boudinaged. Some veins are at a small angle to the foliation and the boudins are asymmetric and supply a top-NNE sense of shear. Still other veins are almost perpendicular to the foliation and are folded. Christine Kumerics used these material markers for strain analysis and a quantitative assessment of the non-coaxiality of deformation (Kumerics et al. 2005).

Figure 34. Three examples of deformed pegmatite

Three examples of deformed pegmatite. (top) Relatively thick foliation-parallel pegmatite layer in the middle of the photograph is stretched in the NNE direction and shows a number of Riedel shears just above cap of felt pen. The pegmatite below is boudinaged and asymmetry of boudinage also indicates top-NNE shear. Note that in the upper right-hand corner the small pegmatite vein is almost perpendicular to the foliation. (middle) Sheared pegmatite with large tourmaline crystals. (bottom) Wide pegmatite veins perpendicular to the foliation. Note that there is a subhorizontal, foliation-parallel pegmatite veins in the middle of the photograph.

Stop 2.6: Mylonitic pegmatite

Drive further east until you reach a valley. Go down into the creek and walk up-stream. There are a number of pegmatites exposed in the creek. The mylonitic metapegmatite sample IK02-4 (Figure 35) is from an outcrop right in the creek bed. The pegmatite is a whitish-yellowish rock with up to 1-2 cm big tourmaline and white mica crystals. As summarised above, Rb/Sr analysis did not succeed in dating mylonitic deformation of this sample. Rather, the large white mica crystals on the mylonitic foliation planes yielded ages of up to 458±7 Ma, which are considered as a minimum age for protolith crystallisation. We believe that the large white mica crystals are actually about 550 Ma old and relate to a Pan-African magmatic event.

Figure 35. Mylonitically deformed pegmatite

(top) Photograph of mylonitically deformed pegmatite sample IK02. (bottom) Mylonitically deformed pegmatite from a locality directly adjacent to that of IK02.

The 40Ar/39Ar ages of IK02-4 range from 13.8±4.8 to 5.4±1.8 Ma and have a weighted mean age of 10.8±1.1 Ma

(2σ errors). The ages from IK02-8 range from 11.1±0.3 to 9.5±0.5 Ma and show a weighted mean age of 10.5±2.4 Ma. We interpret the ages to date phengite recrystallisation during ductile deformation in the Messaria shear zone.

Day 3: Ikaria nappe

Drive from Kampos via Evdilos along the main road to the east. Numerous, variably oriented and deformed pegmatite dikes occur in metapelite of the Ikaria nappe in numerous roadcuts. Metapelite of the Ikaria nappe frequently contains garnet, kyanite and staurolite.

Before the road turns inland and climbs up, have a look back to the SW. There is a distinct difference in the morphology across the Messaria detachment: the marbles and phyllites of the Messaria nappe have a rugged morphology whereas the metapelite of the Ikaria nappe is much less dissected.

Stop 3.1: Kyanite-staurolite-biotite schist

A good outcrop containing kyanite and staurolite occurs on the right hand side of the road in a sharp bend just before Mileopori. In this outcrop, metapelite has the general paragenesis staurolite-biotite-plagioclase-kyanite-chlorite (Figure 32b). The rocks are distinctly foliated and stretched with the typical NNE trend of the extension lineation. Plagioclase often forms porphyroclasts and the penetrative foliation wraps around them. Staurolite and kyanite commonly grew in this foliation.

Plagioclase has andesine composition and shows a zonation from An43 (core) to An50 (rim). Kyanite occurs in plagioclase, and in textural equilibrium with staurolite, plagioclase and biotite in the matrix. Rare chlorite is in equilibrium with biotite and staurolite. The Mg content of chlorite is ~3 per formulae unit (based on 14-oxygen structural formula) and therefore we consider chlorite to be primary. Staurolite is widespread in the matrix, and also forms inclusions in plagioclase. The Si content in white mica varies from 3.10 to 3.15 (on the basis of 11-oxygen structural formula).

P-T estimates for IK02-16 are well constrained because the bulk-rock composition of this sample allows the paragenesis staurolite-biotite, but not the paragenesis garnet-biotite-staurolite. This implies a pressure <7 kbar (Figure 11b). Another indication for pressures <7 kbar is the chlorite-biotite-staurolite paragenesis, which is likely metastable in this sample (Figure 11b). The stable field for this paragenesis is near the staurolite-biotite trivariant field at pressures <7 kbar. Because kyanite is present, pressures are >6 kbar for a temperature of 600°C.

As stated already above, a very important conclusion is that there is no evidence for any high-pressure metamorphism pre-dating amphibolite-facies metamorphism in this and other samples from the Ikaria nappe.

A bit further up the road about 1 km W of Ploumarion you will find garnet-bearing schist in the road cuts. The main foliation wraps around the garnets and top-NNE shear bands occur. The development of the shear bands clearly postdates garnet growth.

Stop 3.2: Deformed Xylosirtis S-type granite on the crest of the island

Continue driving uphill to the east. When you almost reached the crest of the island there is a turnoff to the right. The dirt road brings you further up the mountains towards a transmitter station. Keep going towards the southwest along the crest of the hill. The road is usually pretty bad. If you worry about your vehicle, park it and walk. You will see the whitish S-type Xylosirtis granite when you look down to the south coast. The granite crops out along the main road at the south coast and also makes up a large part of the southern slopes of Ikaria's central part. About 100-200 m below the footpath along the crest of the island you will see the contact between the Xylosirtis granite and metapelite of the Ikaria nappe. There are a bunch of goat tracks that bring you to the contact zone. The latter is marked by mylonitically deformed granite and metapelite. Both rocks types are penetratively foliated and contain a pervasive NNE-trending stretching lineation.

Go back to the main road, take a right and drive down towards Agios Kirikos. A few kilometeres before you reach Agios Kirikos, bear right towards Xylosirtis and Chrisostomos.

Stop 3.3: Mildly deformed Xylosirtis granite

From the main road at the south coast you will see the whitish Xylosirtis granite in the mountainous slopes above the road. Almost everywhere along the road the granite is mildly deformed and hardly exhibits a tectonic foliation.

Stop 3.4: Garnet-staurolite schist

Continue along the main road towards Xylosirtis. When you get out of the granite proper you will find a contact zone in which metapelite of the Ikaria nappe and granite dikes are interleaved and both are quite strongly deformed together. There a clear intrusive relationships between the granite and the metapelite. Before you reach Xylosirtis there is a garnet-staurolite-bearing metapelite outcrop on

the right hand side of the road in a creek bed. The rock shows big plagioclase and garnet crystals and occasionally top-NNE shear bands which wrap around the plagioclase and garnet.

Sample IK02-06a from this outcrop contains the mineral assemblage garnet, staurolite, biotite and rare epidote (+ muscovite + quartz) (Figure 32a). Garnet has a general grain size of about 3 mm and its composition is almandine (70-73%), pyrope (5-10%), spessartine (5-10%) and grossular (12-18%). Garnet has no major element zoning, mineral formulae do not show significant Fe3+ and therefore we assumed that Fe2+ = Fetotal. Staurolite occurs, together with chlorite, as inclusions in garnet or in the matrix in equilibrium with biotite and garnet. Epidote also forms inclusions in garnet or is common in the matrix in equilibrium with biotite. Chlorite only occurs as inclusions in garnet. The Si content of white mica in the matrix is 3.11-3.12 (on the basis of 11-oxygen structural formula).

T he pseudosection and AFM projections (Figure 11) constrain P-T estimates for IK02-06a at 6-8 kbar for a temperature of 600-650°C. Isopleths of phengitic substitution do not provide precise information on pressure but suggest that the maximum pressure was <8 kbar. The size of garnet (3 mm) does not allow any significant fractionation of the whole-rock composition. Because chlorite and staurolite occur as inclusions in garnet, the P-T path is probably clockwise (Figure 11a).

Stop 3.5: Marbles of Ikaria nappe

If you are keen to explore the south coast a bit further, continue going west towards Plagia. Before you reach Chrisostamos you will be in whitish-yellowish, coarse-crystalline, dolomitic marble of the Ikaria nappe. Locally this marble is referred to as the Nikaria marble. The marble is distinctly coarser grained the any marble of the Messaria nappe and also distinctly lighter in colour.

Go back to Agios Kirikos and spend the night there. Agios Kirikos is built on rocks of the Messaria nappe and intercalations of phyllite and marble dominate the hills around the town.

Day 4: Messaria and Fanari nappe in the east

Take the road from Agios Kirikos towards the airport. This road to the airport used to be a very narrow road but was considerably improved and distinctly widened when we did field work on Ikaria. Road construction caused a number of new and fresh outcrops but may have meanwhile destroyed the outcrop described below.

Stop 4.2: Therma

It is worthwhile to pay the town of Therma a visit. Since ancient times Therma is known for its therapeutic radon hot mineral springs. The hot springs aid in the curing of a multitude of afflictions such as rheumatism, arthritis, neuralgia, and infertility. The essential elements in Ikaria's therapeutic hot mineral springs are saline radium and radonium. It is the main spa town of Ikaria. The village feast is held on 1 July, the day of Agia Anargiri.

The name Therma is from the ancient Ikarian town of Thermae. In bygone days the inhabitants of Thermae were known as Asclipians from the god of medicine (Asclipios) and in recognition for their miracle working hot springs. At a small distance east of the present day town at the location "Xalasmena Therma" stand the ruins of the ancient spa. It was a seaside town built on a small projecting peninsula and was one of the known spas of ancient times. This is proven by the fragments of broken marble bath tubs found in the area and traces of an ancient aqueduct partly hollowed out in the rocks. Unfortunately it is not known exactly when this ancient town was inhabited. However, from a marble Stele found in the area we know that the town existed and flourished in the classical era and was a member of the Athenian Naval League. Its disappearance, probably due to an earthquake circa 205 B.C., did not allow for more information to come to the surface about the life of the Thermaen people. Although no archaeological research has been carried out it is believed that the seacoast where Xalasmena Thermae is situated is the exact location of the ancient city of Thermae.

Stop 4.2: Cataclasite at base of Fanari nappe

You drive in massive grey marble of the Messaria nappe and towards the airport this marble is becoming increasingly brittlely deformed. Because of the extensive roadworks the outcrop situation has changed considerably but you should be able to find extremely cataclastically reworked marble in the roadcuts around Panagia. The brittle deformation of the dark-grey marble of the Messaria nappe transformed the latter into a blackish, clay-bearing cataclastic rock. The cataclasite is foliated and contains numerous Riedel shears.

Stop 4.3: Conglomerate of Fanari nappe

Before you reach the airport there is a turnoff to your right towards Fanari. When you enter Fanari from the west, bear left and try to find a road that brings you to the eastern side of the valley, this is the road to the tower of Fanari.

You will drive below the runway of Ikaria airport and then the road climbs slightly up to the south and southeast.

The Pliocene conglomerates of the Fanari nappe (Figure 28), which is part of the Upper unit of the Cycladic zone, contain pebbles of metamorphic rocks, which are not exposed on Ikaria Island. Abundant are amphibolite pebbles, marble is also ubiquitous. In addition a number of volcanic clasts occur, as do metapelite and quartzite pebbles.

Stop 4.4: Dracanum

Continue to the east on this dirt road until the road ends; from there it is a 10 min hike to the tower of Dracanum (Figure 2), which is a must-see on Ikaria. The tower is one of the best preserved Hellenistic military towers in the Aegean.

Turn around and go back via Fanari to the main road, take a right there, pass the main airport building and hit a dirt road that turns west after the airport. You are in grey marble of the Messaria nappe. This road brings you up to the crest of the island. After about 1 km WSW of the airport you will cross the contact between the Messaria and the Ikaria nappe. There are a number of good outcrops in the road cuts to your left. Go back up to the main road and then take a left down to Agios Kirikos.

Acknowledgements

My various visits to Ikaria were always a great joy, particularly because of Vassilis´ hospitality. I would also like to thank students from Mainz University for mapping the central part of the island in detail, one of them, Markus Diehl, kindly provided numerous photographs, which Anekant Wandres from our department scanned in and assembled.

References

Altherr, R., Kreuzer, H., Wendt, I., Lenz, H., Wagner, G.A., Keller, J., Harre, W. & Höhndorf, A. 1982. A late Oligocene/early Miocene high temperature belt in the Attic-Cycladic crystalline complex (SE Pelagonian, Greece). Geologisches Jahrbuch, E23, 97-164.

Altherr, R., Kreuzer, H., Lenz, H., Wendt, I., Harre, W. & Dürr, S. 1994. Further evidence for a late Cretaceous low-pressure/ high-temperature terrane in the Cyclades, Greece. Chemie der Erde, 54, 319-328.

Avigad, D. & Garfunkel, T. 1989. Low-angle faults above and below a blueschist belt, Tinos Island, Cyclades, Greece. Terra Nova, 1, 182-187.

Buick, I.S. 1991. Mylonite fabric development on Naxos, Greece. Journal of Structural Geology, 13, 643-655.

Dürr, S., Altherr, R., Keller, J., Okrusch, M. & Seidel, E. 1978. The Median Aegean Crystalline Belt: Stratigraphy, structure, metamorphism, magmatism. In: Alps, Apennines, Hellenides, Cloos, H., Roeder, D. & Schmidt, K., E. Schweizerbart'sche Verlagsbuchhandlung, Stuttgart, 455-477.

Faure, M., Bonneau, M. & Pons, J. 1991. Ductile deformation and syntectonic granite emplacement during the late Miocene extension of the Aegean (Greece). Bulletin de la Société Géologique de France, 162, 3-11.

Fytikas, M., Innocenti, F., Manetti, P., Mazzuoli, R., Peccerillo, A. & Villari, L. 1984. Tertiary to Quaternary evolution of volcanism in the Aegean region. In: The geological evolution of the eastern Mediterranean (eds A.H.F. Robertson and J.E. Dixon). Geological Society of London, Special Publications, 17, 687-699.

Gessner, K., Ring, U., Passchier, C.W. & Güngör, T. 2001. How to resist subduction: Eocene post-high-pressure emplacement of the Cycladic blueschist unit onto the Menderes nappes, Anatolide belt, western Turkey. Journal of Geological Society of London, 158, 769-780.

Gessner, K., Collins, A.S., Ring, U. & Güngör, T. 2004. Structural and thermal history of poly-orogenic basement: U-Pb geochronology of granitoid rocks in the southern Menderes Massif, Western Turkey. Journal Geological Society London, 161, 93-101.

Godfriaux, I. 1968. Etude géologique de la région de l'Olympe (Gréce). Annales Géologiques des Pays Helleniques, 19, 1-271.

Keay, S.M. 1998. The geological evolution of the Cyclades, Greece: constraints from SHRIMP U-Pb geochronology. PhD thesis, Australian National University, Canberra.

Kumerics, C., Ring, U., Brichau, S., Glodny, J. & Monié, P. 2005. The extensional Messaria shear zone and associated brittle detachment faults, Aegean Sea, Greece. Geological Society of London, 162, 701-721.

Lee, J. & Lister, G.S. 1992. Late Miocene ductile extension and detachment faulting, Mykonos, Greece. Geology, 20, 121-124.

Lister, G.S., Banga, G. & Feenstra, A. 1984. Metamorphic core complexes of Cordilleran type in the Cyclades, Aegean Sea, Greece. Geology, 12, 221-225.

Lister, G.S. & Baldwin, S.L. 1993. Plutonism and the origin of metamorphic core complexes. Geology, 21, 607-610.

Régnier, J.L., Ring, U., Passchier, C.W., Gessner, K. & Güngör, T. 2003. Contrasting metamorphic evolution of metasedimentary rocks from the Çine and Selimiye nappes in the Anatolide belt, western Turkey. Journal of Metamorphic Geology, 21, 1-23.

Ring, U., Buchwaldt, R. & Gessner, K. 2004. Pb/Pb dating of garnet from the Anatolide belt in western Turkey: Pan-African metamorphism related to the collision of Angara with Gondwana. Zeitschrift Deutsche Geologische Gesellschaft, 154, 537-555.

Ring, U., Gessner, K., Güngör, T. & Passchier, C.W. 1999a. The Menderes Massif of western Turkey and the Cycladic Massif in the Aegean - do they really correlate? Journal Geological Society London, 156, 3-6.

Ring, U. & Layer, P.W. 2003. High-pressure metamorphism in the Aegean, eastern Mediterranean: Underplating and exhumation from the Late Cretaceous until the Miocene to Recent above the retreating Hellenic subduction zone. Tectonics, 22, 1022, doi: 10.1029/2001ITC001350, 23 p.

Ring, U., Laws, S. & Bernet, M. 1999b. Structural analysis of a complex nappe sequence and late-orogenic basins from the Aegean Island of Samos, Greece. Journal of Structural Geology, 21, 1575-1601.

Ring, U. & Reischmann, T. 2002. The weak and superfast Cretan detachment, Greece: exhumation at subduction rates in extruding wedges. Journal of the Geological Society of London, 159, 225-228.

Ring, U., Willner, A.P. & Lackmann, W. 2001. Stacking of nappes with unrelated pressure-temperature paths: an example from the Menderes nappes of western Turkey. American Journal of Science, 301, 912-944.

Robertson, A.H.F., Clift, P., Degnan, P.J. & Jones, G. 1991. Palaeogeographic and palaeotectonic evolution of the Eastern Mediterranean Neotethys. Palaeogeography, Palaeoclimatology, Palaeoecology, 87, 289-343.

Tomaschek, F., Kennedy, A., Villa, I.M. & Ballhaus, C. 2003. Zircons from Syros, Cyclades, Greece - Recrystallization and mobilisation during high pressure metamorphism. Journal of Petrology, 44, 1977-2002.

Vandenberg, L.C. & Lister, G.S. 1996. Structural analysis of basement tectonites from the Aegean metamorphic core complex of Ios, Cyclades, Greece. Journal of Structural Geology, 18, 1437-1454.

Weidmann, M., Solounias, N., Drake, R.E. & Curtis, G.H. 1984. Neogene stratigraphy of eastern basin, Samos Island, Greece. Geobios, 17, 477-490.

Wijbrans, J.R., Schliestedt, M. & York, D. 1990. Single grain argon laser probe dating of phengites from the blueschist to greenschist transition on Sifnos (Cyclades, Greece). Contributions to Mineralogy and Petrology, 104, 582-593.

Will, T., Okrusch, M., Schmädicke, E. & Chen, G. 1998. Phase relations in the greenschist-blueschist-amphibolite-eclogite facies in the system Na2O-CaO-FeO-MgO-Al2O3-SiO2-H2O (NCFMASH), with application to metamorphic rocks from Samos, Greece. Contributions to Mineralogy and Petrology, 132, 85-102.

Error: no bibliography entry: d0e1006 found in http://docbook.sourceforge.net/release/bibliography/bibliography.xml